



Preliminary clinical experience with a robot-assisted system in preoperative hookwire localization of pulmonary nodules: a prospective pilot study

Li Pengfei¹ · Zheng Wenheng² · Wang Zheng¹ · Zhang Xueling³ · Tong Zhuang¹ · Zhang Liang¹ · Yao Hehuan¹ · Zhang Chenlei¹ · Wang Gebang¹ · Liu Yu¹ · Liu Zheyu¹ · Ma Yegang¹ · Xie Weiguo³ · Huang Bingding⁴ · Liu Hongxu¹

Received: 14 August 2025 / Accepted: 18 September 2025
© The Author(s) 2025

Abstract

Accurate preoperative localization is critical for the surgical resection of small pulmonary nodules, yet conventional CT-guided hookwire placement remains operator-dependent and technically demanding. This prospective study evaluated the clinical performance of a robot-assisted navigation system for CT-guided preoperative hookwire localization of pulmonary nodules. The trial enrolled 60 patients scheduled for localization followed by VATS. Primary endpoints included first-attempt puncture success rate, needle placement accuracy, localization success rate, procedure duration, number of punctures, radiation dose, and complication rate, with subgroup analyses by lesion characteristic and patient positioning. The first-attempt puncture success rate was 100.0%, with an median needle placement accuracy of 5.7 mm (IQR 4.2–7.9). Localization success was achieved in 94.8% of nodules (55/58). The median procedure duration was 16.6 min (14.0–22.9), and the median radiation dose was 281.2 mGy·cm (227.1–365.8). The overall complication rate was 5.2% (3/58). Accuracy was consistent across subgroups, although lower lobe lesions and prone positioning were associated with longer procedure times, and prone positioning also increased radiation exposure, without compromising accuracy. These findings demonstrate the feasibility, precision, and safety of this system, supporting its potential to standardize and improve preoperative localization in thoracic surgery. *Trial registration:* Registry: <https://www.chictr.org.cn/>, TRN: ChiCTR2500095919, Registration date: January 15, 2025.

Keywords Pulmonary nodules · Hookwire preoperative localization · CT-guided percutaneous

Pengfei Li, Wenheng Zheng and Zheng Wang have contributed equally to this work.

✉ Huang Bingding
huangbingding@sztu.edu.cn

✉ Liu Hongxu
liuhongxu3366@163.com

¹ Department of Thoracic Surgery, Liaoning Cancer Hospital & Institute, Cancer Hospital of Dalian University of Technology, Cancer Hospital of China Medical University, Shenyang 110042, China

² Department of Interventional Radiology, Liaoning Cancer Hospital & Institute, Cancer Hospital of Dalian University of Technology, Cancer Hospital of China Medical University, Shenyang 110042, China

³ Würzburg Dynamics Ltd., Shenzhen 518000, China

⁴ College of Big Data and Internet, Shenzhen Technology University, Shenzhen 518118, China

Introduction

Video-assisted thoracoscopic surgery (VATS) has high sensitivity and specificity for diagnosis and treatment of suspicious pulmonary nodules [1]. However, it is limited in localizing small, deep, or ground-glass nodules, which are often difficult to visualize or palpate intraoperatively [2, 3]. Failure to localize pulmonary nodules < 1 cm during VATS has been documented in up to 16.1% of cases, and this technical limitation has been associated with conversion rates to open thoracotomy as high as 54% [4, 5].

Several preoperative localization techniques have been developed to improve VATS success. Conventional CT-guided techniques can be categorized into liquid marker injection and metallic device placement, both achieving high technical success rates. An emerging minimally invasive approach, electromagnetic navigation bronchoscopy (ENB) with dye marking or fiducial placement, further improve

accuracy and reduce complications [6]. Notably, technique selection should consider availability, nodule features, comorbidities, and pulmonary function [6]. Among these methods, hookwire localization is one of the most commonly used methods, offering reliable intraoperative visual guidance for nodule resection [7, 8].

In recent years, robot-assisted navigation systems have demonstrated promising feasibility, safety, and accuracy in percutaneous lung biopsy [9–11]. Their application has extended to the preoperative localization of nodules via injection of indocyanine green (ICG) [12, 13]. A recently retrospective study also reported the efficacy and safety of robot-assisted CT-guided hookwire localization [14]. However, prospective evidence evaluating the clinical performance of such systems in hookwire localization remains

limited. This prospective study aims to evaluate the clinical performance and potential advantages of a robot-assisted navigation system for CT-guided hookwire preoperative localization of pulmonary nodules.

Materials and methods

Patient selection

This single-arm prospective trial was conducted at Liaoning Cancer Hospital & Institute (Cancer Hospital of Dalian University of Technology) from April 2024 to June 2024, enrolling 60 patients with pulmonary nodules based on predefined inclusion and exclusion criteria (Fig. 1). Inclusion

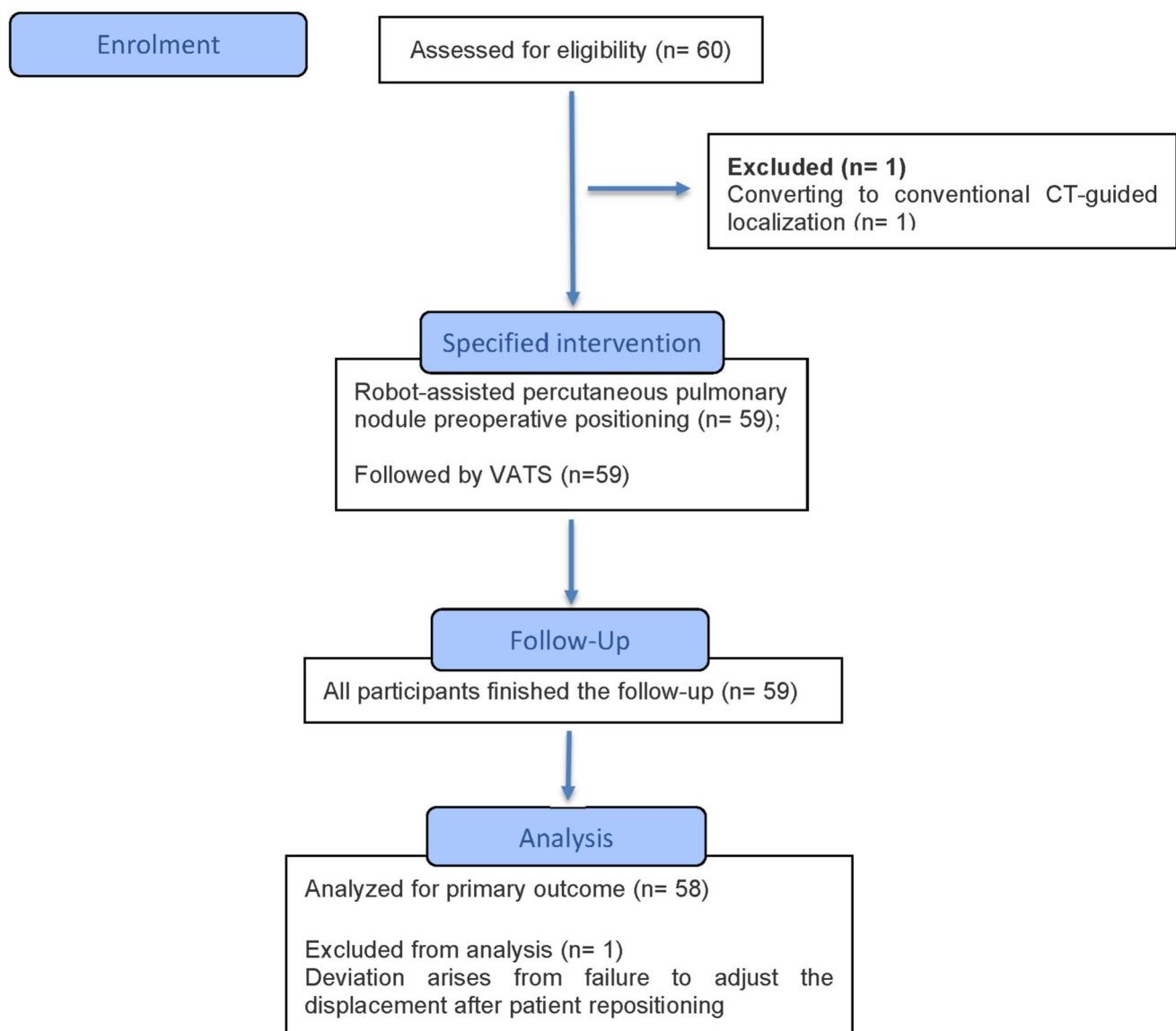


Fig. 1 Flowchart of study design

criteria were: (1) aged 18–80 years; and at least one of the following: (2a) solitary peripheral nodule < 10 mm and > 15 mm from the pleural [2]; (2b) pure ground-glass and part-solid nodules on imaging; or (2c) nodules deemed difficult to localize intraoperatively. Exclusion criteria included: (1) uncorrectable or significant coagulation abnormalities; (2) inaccessible or high risk lesion; and (3) severe cardiopulmonary, hepatic, or renal dysfunction. The trial was approved by the Ethics Committee of Liaoning Cancer Hospital & Institute (Approval No. 20240410) on April 9, 2024. All participants provided written informed consent in accordance with the Declaration of Helsinki.

Robot-assisted hookwire localization procedures

Robot-assisted CT-guided lung punctures were performed by two interventional radiologists, who had completed standardized training before study initiation, using a navigation system (Wuerzburg Dynamics Ltd., Shenzhen, China) and a 100×0.9 mm hookwire device (Nanjing Polymer Medical Technology Co., Ltd., Nanjing, China).

Optical markers were placed on the chest and abdomen (Fig. 2a), and a breath-hold CT scan was acquired for 3D reconstruction of skin, bones, and vasculature (Fig. 2b). The operator selected puncture targets and entry points, and the system automatically verified trajectories to avoid critical structures. After sterile preparation, the robotic arm aligned the guiding apparatus with the planned trajectory (Fig. 2c, d). Punctures were performed during breath-holding, synchronized with real-time respiratory monitoring.

Post-puncture CT scan confirmed needle placement (Fig. 3a, b), defined as ≤ 2 cm from the lesion edge. Upon confirmation, the hookwire was deployed and the sheath withdrawn; unsuccessful attempts were corrected under CT

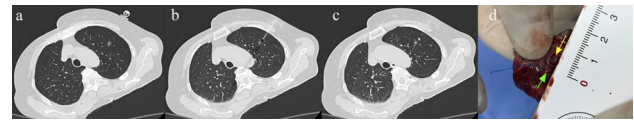


Fig. 3 CT images before and after the puncture, and the resected lung tissue from a representative case. **a** Pre-puncture CT image, **b** Post-puncture CT image showing successful first-attempt puncture with the initial needle, and **c** Final thoracic CT image with the marker placed at the target site and no complications observed; **d** Resected lung tissue following surgery, with the distance measured between the localization marker and the lesion. Yellow arrow: lesion; Green arrow: localization marker.

guidance. A final CT verified marker position and assessed for any complications (Fig. 3c).

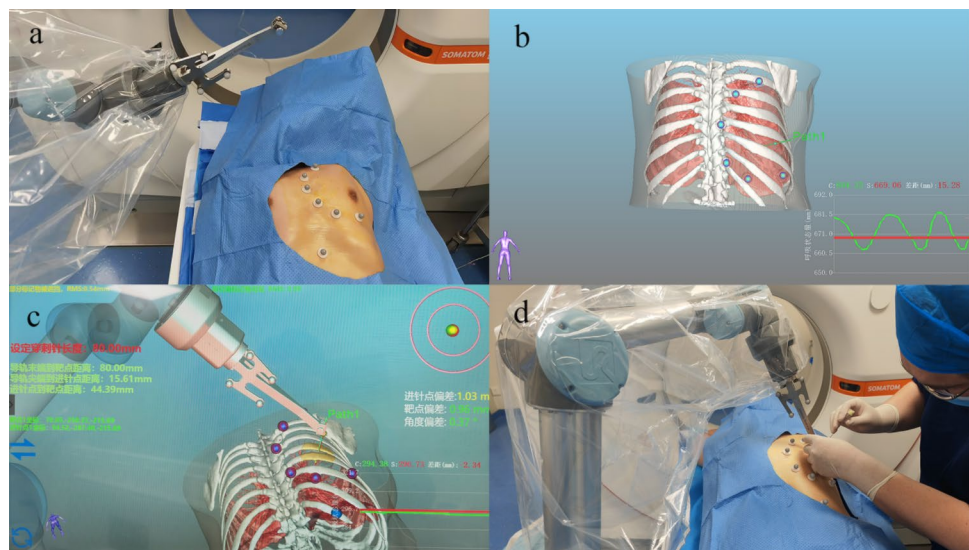
Patients were transferred to the operating room in within 24 h. Surgical resections were subsequently performed by senior thoracic surgeons with professional titles of Associate Chief Physician or above.

Outcome measurements

The primary endpoint was the first-attempt puncture success rate, defined as the proportion of successful punctures achieved on the initial needle insertion. Secondary endpoints included: (1) Needle placement accuracy: 3D distance between planned target and actual needle tip; (2) Localization success rate: the proportion of marker-to-lesion distance ≤ 2 cm in the resected specimen (Fig. 3d); (3) Procedure duration: calculated from the start of the first CT scan to the CT-confirmed satisfactory placement of the localization marker; (4) Number of punctures: including trajectory adjustments; (5) Radiation dose; (6) Surgical outcomes.

Safety was evaluated based on the incidence of complications occurring from the time of informed consent to the

Fig. 2 Schematic workflow of the robot-assisted percutaneous lung puncture procedure. **a** Placement of optical markers on the chest and abdomen, followed by CT scanning, **b** 3D reconstruction of the lung anatomy, **c** Path planning and navigation setup, and **d** Needle puncture guided by the robotic system.



end of follow-up after VATS. Adverse events were graded according to the Common Terminology Criteria for Adverse Events (CTCAE) Version 5.0.

Statistical analyses

Statistical analysis was conducted using the SPSS software (Version 26.0, SPSS Inc.). Continuous variables were expressed as mean \pm SD or median (IQR), and categorical variables as counts and percentages. Subgroup analyses were performed by lesion characteristics and patient position. Depending on data distribution, comparisons were made using the Kruskal–Wallis test, Mann–Whitney *U* test, or *t*-test. All statistical tests were two-sided, with *P*-value < 0.05 considered statistically significant.

Results

A total of 60 patients were enrolled, two patients were excluded from the final analysis: one due to significant deviation caused by uncorrected displacement after patient repositioning, and one due to conversion to conventional CT-guided localization for inadequate breath-hold control.

The final cohort included 58 patients (19 males and 39 females) with a mean age of 59.8 ± 8.4 years and a median body mass index (BMI) of 23.5 kg/m^2 (IQR: 21.8–26.3). None of the patients had comorbidities, and two had a history of thoracic surgery or radiotherapy. Median nodule diameters was 9.0 mm (7.4–12.6), and median pleural distance 10.0 mm (1.9–15.8). Distribution by lobe was: right upper lung (20/58, 34.5%), right middle lobe (8/58, 13.8%), right lower lobe (8/58, 13.8%), left upper lobe (15/58, 25.9%), and left lower lobe (7/58, 12.1%). Nodule types included solid nodule (12/58, 20.7%), part-solid ground-glass (21/58, 36.2%), and pure ground-glass (25/58, 43.1%) (Table 1).

All 58 patients successfully underwent surgical resection, including wedge resection in 44 (75.9%), segmentectomy in 10 (17.2%), and lobectomy in 4 (6.9%) patients (Table 2). First-attempt puncture success rate was 100% (58/58). Localization success rate was 94.8% (55/58), with failures due to marker displacement ($n = 1$), dislodgement ($n = 1$), and inconclusive localization from ground-glass opacity with bleeding ($n = 1$). Median needle placement accuracy was 5.7 mm (4.2–7.9), median procedure duration 16.6 min (14.0–22.9), radiation dose $281.2 \text{ mGy}\cdot\text{cm}$ (227.1–365.8), and mean puncture depth 57.0 ± 17.4 mm. Most were performed supine (36/58, 62.1%) or prone (20/58, 34.5%).

Subgroup analyses (Table 3) showed no significant differences in accuracy, duration, or radiation dose between lesions < 10 mm vs ≥ 10 mm (accuracy 95% CI $- 2.80, 0.70, P = 0.232$; duration $Z = - 1.05, P = 0.295$;

Table 1 Demographic and clinical characteristics of the study population and pulmonary nodules ($N = 58$)

Characteristics	Value
Age (years), mean \pm SD	59.8 ± 8.4
Gender, n (%)	
Male	19 (32.8)
Female	39 (67.2)
BMI (kg/m^2)	$23.5 (21.8\text{--}26.3)$
Comorbidities, n (%)	
Yes	0 (0)
No	58 (100)
History of thoracic surgery or radiotherapy, n (%)	
Yes	2 (3.4)
No	56 (96.6)
Lesion size (mm), median (IQR)	$9.0 (7.4\text{--}12.6)$
Distance from pleural surface (mm), median (IQR)	$10.0 (1.9\text{--}15.8)$
Location, n (%)	
Right lung	36 (62.1)
Upper lobe	20 (34.5)
Middle lobe	8 (13.8)
Lower lobe	8 (13.8)
Left lung	22 (37.9)
Upper lobe	15 (25.9)
Lower lobe	7 (12.1)
Nodule type, n (%)	
Solid	12 (20.7)
Part-solid ground-glass	21 (36.2)
Pure ground-glass	25 (43.1)

IQR Interquartile range, SD Standard deviation

dose $Z = - 0.83, P = 0.407$) or pleural distance ≤ 15 mm vs > 15 mm (accuracy $Z = - 0.22, P = 0.824$; duration $Z = - 1.57, P = 0.116$; dose $Z = - 0.04, P = 0.966$). Lower lobe lesions and prone positioning prolonged procedure time (location $\chi^2 = 13.37, P = 0.001$; position $Z = - 2.82, P = 0.005$), and prone positioning increased radiation dose ($Z = - 2.05, P = 0.040$) as well, while accuracy remained unaffected ($P > 0.05$). Nodule type (solid vs subsolid) was not associated with any outcome (all $P > 0.05$).

Complications occurred in 5.2% (3/58) of patients, all grade 1–2: pneumothorax requiring drainage ($n = 1$) and hemorrhage managed with hemostatic agents ($n = 1$) or observation ($n = 1$). No other adverse events were observed.

Discussion

The ideal preoperative localization technique for VATS should provide high accuracy, low complication rates, minimal invasiveness. More recently, robotic-assisted localization has demonstrated superior accuracy and lower

Table 2 Procedure outcomes (N = 58)

Outcomes	Value
Puncture depth (mm), mean \pm SD	57.0 \pm 17.4
Patient position, n (%)	
Supine	36 (62.1)
Lateral	2 (3.4)
Prone	20 (34.5)
First-attempt puncture success rate (%)	100.0
Needle placement accuracy (mm), median (IQR)	5.7 (4.2–7.9)
Localization success rate (%)	94.8
Procedure duration (min), median (IQR)	16.6 (14.0–22.9)
Number of punctures (n), median (IQR)	1.0 (1.0–1.0)
Radiation dose (mGy·cm), median (IQR)	281.2 (227.1–365.8)
Complications, n (%)	3 (5.2)
Pneumothorax	1 (1.7)
Hemorrhage	2 (3.4)
Others	0 (0.0)
Surgical outcomes, n (%)	
Wedge resection	44 (75.9)
Segmentectomy	10 (17.2)
Lobectomy	4 (6.9)

mGy·cm Milligray centimeter

complication rates compared with conventional methods [13, 15]. The robotic system applied in this study combines optical tracking, CT-based 3D reconstruction, and an automated robotic arm, which streamline the procedure and improve the success of percutaneous puncture [10].

Conventional hookwire localization shows a pooled success rate of 91.6%, procedure duration of 14.9–23.9 min, mean radiation exposure of 578.71 mGy·cm at 120 kV, complication rates of 13.5–37.8%, and hookwire dislodgement rates of 8–47% [3, 16–22]. In our study, robotic navigation achieved a higher localization success rate (94.8%), comparable procedure times (16.6 min), substantially lower radiation dose (281.2 mGy·cm) and a lower complication rate (5.2%), which may be attributed to improved needle placement accuracy (median 5.7 mm) and the absence of trajectory adjustment. However, standardized randomized controlled trials are needed to validate these performance differences. In a previous study using a different robotic system, first-attempt success rates were similarly high (100%), but procedure times were longer (25.0 min) and radiation exposure was higher (1491.0 mGy·cm), likely due to differences in CT protocols [13]. Emerging reports support

the growing role of robotic assistance in VATS localization [12–14].

In this study, we evaluated factors affecting robotic-assisted hookwire puncture performance, focusing on lesion characteristics and patient positioning. Regarding lesion characteristics, nodule size (< 10 mm) and pleural distance (> 15 mm), which are commonly cited as key determinants for successful intraoperative identification during conventional VATS [2, 23], did not significantly influence robotic-assisted performance metrics such as needle placement accuracy, procedure duration, or radiation dose. Similarly, no significant differences were observed in puncture performance between solid and sub-solid nodules. In fact, solid component influences biopsy diagnostic accuracy instead of robotic-assisted targeting [24]. Concerning patient and procedural factors, lower-lobe lesions and procedures performed in the prone position were associated with longer procedure times, likely due to increased respiratory motion [25], but these factors did not compromise needle placement accuracy. These findings demonstrate that robotic navigation systems provide reliable and precise access to pulmonary nodules regardless of lesion characteristics or patient positioning.

Although this study evaluated robotic assistance only for CT-guided percutaneous localization, it may also be applicable to ENB-guided approaches, which has been shown promise in VATS nodule localization with reduced invasiveness and complication risk [26–28]. In bronchoscopic biopsy, robotic-assisted bronchoscopy (RAB) has been shown to improve diagnostic accuracy through virtual navigation [29]. While clinical evidence for its efficacy and safety in preoperative localization is still limited, growing experience with ENB-guided techniques indicates potential clinical value. However, concerns remain regarding the widespread adoption of robotic assistance in clinical practice, including high cost and the need for specialized training [30]. In this initial clinical application, high precision and efficiency were achieved after standard training on 3–4 patients, indicating a shortened learning curve and potential value for clinical practice.

However, the generalizability of these findings is limited by the single-center, single-arm design and small sample size, highlighting the need for validation in a large, multi-center randomized trial. In conclusion, this pilot study demonstrates the feasibility and safety of a robotic-assisted navigation system for preoperative hookwire localization of pulmonary nodules across diverse clinical scenarios. These findings highlight the potential of robotic systems to improve procedural standardization and reduce operator dependence in VATS preoperative localization.

Table 3 Subgroup analysis of procedure outcomes

Variables	n (%) ^b	Needle placement accuracy (mm) ^a	Procedure duration (min) ^a	Radiation dose (mGy·cm) ^a
Lesion size (mm)				
< 10 mm	32 (55.2)	5.8 ± 2.5	15.7 (14.0–21.5)	267.5 (199.0–368.3)
≥ 10 mm	26 (44.8)	6.8 ± 3.8	17.4 (14.2–28.2)	293.3 (239.5–359.1)
Statistic values	/	– 2.80, 0.70	– 1.05	– 0.83
P-value ^c	/	0.232	0.295	0.407
Distance from pleural surface (mm)				
≤ 15 mm	41 (70.7)	5.8 (4.1–7.8)	16.1 (13.9–20.5)	282.0 (219.1–372.4)
> 15 mm	17 (29.3)	5.7 (3.9–9.5)	19.1 (15.0–30.9)	280.3 (237.1–360.0)
Statistic values	/	– 0.22	– 1.57	– 0.04
P-value ^c	/	0.824	0.116	0.966
Lesion location				
Upper lobe	35 (60.3)	5.1 (3.9, 7.6)	14.6 (13.8–18.5)	280.3 (232.4–350.4)
Middle lobe	8(13.8)	6.5 ± 2.9	15.7 (13.9–25.7)	242.0 (174.1–309.5)
Lower lobe	15 (25.9)	6.4 ± 2.3	21.8 (17.7–29.1)	356.2 (211.3–393.1)
Statistic values	/	1.08	13.37	2.87
P-value ^c	/	0.583	0.001	0.238
Nodule type				
Solid	12 (20.7)	6.6 ± 3.1	15.2 (13.9–26.5)	276.5 (245.0–391.7)
Part-solid ground-glass	21 (36.2)	5.4 (4.0–6.5)	19.7 (14.5–29.0)	313.4 (195.3–383.8)
Pure ground-glass	25 (43.1)	6.4 ± 3.5	16.0 (14.0–18.8)	280.3 (219.2–341.5)
Statistic values	/	0.48	4.35	0.68
P-value ^c	/	0.786	0.114	0.712
Patient position				
Supine	36 (62.1)	5.2 (3.9–7.1)	14.8 (13.8–18.9)	260.4 (199.9–341.5)
Lateral	2 (3.4)	N/A ^d	N/A ^d	N/A ^d
Prone	20 (34.5)	6.4 ± 2.6	19.5 (17.1–24.8)	330.0 (248.1–385.7)
Statistic values	/	– 0.98	– 2.82	– 2.05
P-value ^c	/	0.330	0.005	0.040

^aData are presented as median (IQR) or mean ± SD, as appropriate

^bn (%) indicates the number and percentage of patients in each subgroup

^cP-values were calculated using student t test, the *Kruskal–Wallis* test or the *Mann–Whitney U* test, as appropriate, bold values indicate $P < 0.05$

^dN/A, not application due to small sample size

Acknowledgements The authors thank all participants and investigators for their involvement in this study.

Author contributions [Bingding Huang], [Hongxu Liu] and [Pengfei Li] contributed to the study conception and design. Material preparation, data collection and analysis were performed by [Pengfei Li], [Wenheng Zheng], [Zheng Wang] and [Xueling Zhang]. The first draft of the manuscript was written by [Pengfei Li] and [Xueling Zhang], and all authors commented on previous versions of the manuscript. All authors read and approved the final manuscript.

Funding This work was supported by the Shenzhen Science and Technology Program (KJZD20240903095605007), the Liaoning Province Science and Technology Plan Project (2023JH2/101700165), and National Key Research and Development Program (2022YFC2407406).

Data availability No datasets were generated or analysed during the current study.

Declarations

Conflict of interest The authors declare no competing interests.

Ethical approval This study was performed in line with the principles of the Declaration of Helsinki. Approval was granted by the Ethics Committee of Liaoning Cancer Hospital & Institute (April 9, 2024/ Approval No. 20240410).

Consent to participate Informed consent was obtained from all individual participants included in the study.

Consent for publication The authors affirm that human research participants provided informed consent for publication of the images in Figs. 2 and 3, the data in Tables 1, 2 and 3.

Open Access This article is licensed under a Creative Commons Attribution-NonCommercial-NoDerivatives 4.0 International License, which permits any non-commercial use, sharing, distribution and reproduction in any medium or format, as long as you give appropriate credit to the original author(s) and the source, provide a link to the Creative Commons licence, and indicate if you modified the licensed material. You do not have permission under this licence to share adapted material derived from this article or parts of it. The images or other third party material in this article are included in the article's Creative Commons licence, unless indicated otherwise in a credit line to the material. If material is not included in the article's Creative Commons licence and your intended use is not permitted by statutory regulation or exceeds the permitted use, you will need to obtain permission directly from the copyright holder. To view a copy of this licence, visit <http://creativecommons.org/licenses/by-nc-nd/4.0/>.

References

- Zhao G, Yu X, Chen W, Geng G, Li N, Liu H et al (2019) Computed tomography-guided preoperative semi-rigid hook-wire localization of small pulmonary nodules: 74 cases report. *J Cardiothorac Surg* 14:149. <https://doi.org/10.1186/s13019-019-0958-z>
- Ciriaco P, Negri G, Puglisi A, Nicoletti R, Del Maschio A, Zannini P (2004) Video-assisted thoracoscopic surgery for pulmonary nodules: rationale for preoperative computed tomography-guided hookwire localization. *Eur J Cardiothorac Surg* 25:429–433. <https://doi.org/10.1016/j.ejcts.2003.11.036>
- Zhang H, Li Y, Chen X, He Z (2022) Comparison of hook-wire and medical glue for CT-guided preoperative localization of pulmonary nodules. *Front Oncol* 12:922573. <https://doi.org/10.3389/fonc.2022.922573>
- Santini M, Fiorelli A, Messina G, Mazzella A, Accardo M (2015) The feasibility of LigaSure to create intestinal anastomosis: results of ex vivo study. *Surg Innov* 22:266–273. <https://doi.org/10.1177/1553350614547771>
- Luo K, Lin Y, Lin X, Yu X, Wen J, Xi K et al (2017) Localization of peripheral pulmonary lesions to aid surgical resection: a novel approach for electromagnetic navigation bronchoscopic dye marking. *Eur J Cardiothorac Surg* 52:516–521. <https://doi.org/10.1093/ejcts/ezx114>
- Zhang H, Zhang C, Li L, Qi J, Yang GH, Li YQ et al (2025) Small pulmonary nodule localization techniques in the era of lung cancer screening: a narrative review. *Int J Surg* 111:2624–2632. <https://doi.org/10.1097/js9.0000000000002247>
- McDermott S, Fintelmann FJ, Bierhals AJ, Silin DD, Price MC, Ott HC et al (2019) Image-guided preoperative localization of pulmonary nodules for video-assisted and robotically assisted surgery. *Radiographics* 39:1264–1279. <https://doi.org/10.1148/rg.2019180183>
- Li C, Liu B, Jia H, Dong Z, Meng H (2018) Computed tomography-guided hook wire localization facilitates video-assisted thoracoscopic surgery of pulmonary ground-glass nodules. *Thorac Cancer* 9:1145–1150. <https://doi.org/10.1111/1759-7714.12801>
- Modi P, Uppe A (2022) Lung biopsy techniques and clinical significance. In: *StatPearls*. StatPearls Publishing, Treasure Island (FL)
- Li J, Su L, Liu J, Peng Q, Xu R, Cui W et al (2023) Optical navigation robot-assisted puncture system for accurate lung nodule biopsy: an animal study. *Quant Imaging Med Surg* 13:7789–7801. <https://doi.org/10.21037/qims-23-576>
- Giannatiempo S, Carpino G, Petitti T, Zobel BB, Grasso RF, Guglielmelli E (2018) Efficacy and economic impact evaluation of a navigation system for assisted lung biopsy. *Healthc Technol Lett* 5:49–53. <https://doi.org/10.1049/htl.2017.0015>
- Duan X, He R, Jiang Y, Cui F, Wen H, Chen X et al (2023) Robot-assisted navigation for percutaneous localization of peripheral pulmonary nodule: an in vivo swine study. *Quant Imaging Med Surg* 13:8020–8030. <https://doi.org/10.21037/qims-23-716>
- Liu J, Jiang Y, He R, Cui F, Lin Y, Xu K et al (2023) Robotic-assisted navigation system for preoperative lung nodule localization: a pilot study. *Transl Lung Cancer Res* 12:2283–2293. <https://doi.org/10.21037/tlcr-23-493>
- Guo H, Ouyang Z, Li X, Han Y, Tao F, Liu M et al (2024) Robotic-assisted CT-guided percutaneous pulmonary nodules localization by hook-wire needles: a retrospective observational study. *J Thorac Dis* 16:4263–4274. <https://doi.org/10.21037/jtd-24-198>
- Saito Y, Watanabe T, Kanamoto Y, Asami M, Yokote F, Dejima H et al (2022) A pilot study of intraoperative localization of peripheral small pulmonary tumors by cone-beam computed tomography: sandwich marking technique. *J Thorac Dis* 14:2845–2854. <https://doi.org/10.21037/jtd-22-190>
- Wang JL, Xia FF, Dong AH, Lu Y (2022) Comparison between coil and hook-wire localization before video-assisted thoracoscopic surgery for lung nodules: a systematic review and meta-analysis. *Wideochir Inne Tech Maloinwazyjne* 17:441–449. <https://doi.org/10.5114/wiitm.2022.116396>
- Ma Y, Cheng S, Li J, Yuan W, Song Z, Zhang H (2023) Preoperative CT-guided localization of pulmonary nodules with low-dose radiation. *Quant Imaging Med Surg* 13:4295–4304. <https://doi.org/10.21037/qims-22-1362>
- Jin X, Wang T, Chen L, Xing P, Wu X, Shao C et al (2021) Single-stage pulmonary resection via a combination of single hookwire localization and video-assisted thoracoscopic surgery for synchronous multiple pulmonary nodules. *Technol Cancer Res Treat* 20:1–9. <https://doi.org/10.1177/15330338211042511>
- Fan L, Yang H, Yu L, Wang Z, Ye J, Zhao Y et al (2020) Multicenter, prospective, observational study of a novel technique for preoperative pulmonary nodule localization. *J Thorac Cardiovasc Surg* 160:532–539. <https://doi.org/10.1016/j.jtcvs.2019.10.148>
- Yan G, Cheng X, Wu S, Ge Y, Li S, Xuan Y (2022) Clinical value and application of preoperative CT-guided hookwire localization of solitary pulmonary nodules for video-assisted thoracic surgery. *Technol Health Care* 30:459–467. <https://doi.org/10.3233/thc-thc228042>
- Mack MJ, Shennib H, Landreneau RJ, Hazelrigg SR (1993) Techniques for localization of pulmonary nodules for thoracoscopic resection. *J Thorac Cardiovasc Surg* 106:550–553
- Bernard A, The Thorax Group (1996) Resection of pulmonary nodules using video-assisted thoracic surgery. *Ann Thorac Surg* 61:202–204. [https://doi.org/10.1016/0003-4975\(95\)01014-9](https://doi.org/10.1016/0003-4975(95)01014-9)
- Demmy TL, Wagner-Mann CC, James MA, Curtis JJ, Schmaltz RA, Walls JT (1997) Feasibility of mathematical models to predict success in video-assisted thoracic surgery lung nodule excision. *Am J Surg* 174:20–23. [https://doi.org/10.1016/s0002-9610\(97\)00021-4](https://doi.org/10.1016/s0002-9610(97)00021-4)
- Cheng M, Ding R, Wang S (2024) Diagnosis and treatment of high-risk bilateral lung ground-glass opacity nodules. *Asian J Surg* 47:2969–2974. <https://doi.org/10.1016/j.asjsur.2024.01.072>

25. Tan KV, Thomas R, Hardcastle N, Pham D, Kron T, Foroudi F et al (2015) Predictors of respiratory-induced lung tumour motion measured on four-dimensional computed tomography. *Clin Oncol (R Coll Radiol)* 27:197–204. <https://doi.org/10.1016/j.clon.2014.12.001>
26. Marino KA, Sullivan JL, Weksler B (2016) Electromagnetic navigation bronchoscopy for identifying lung nodules for thoroscopic resection. *Ann Thorac Surg* 102:454–457. <https://doi.org/10.1016/j.athoracsur.2016.03.010>
27. Xia T, Li Y, Shen Z, Fang Z, Chen J, Pan S et al (2024) Comparison of safety and anxiety/depression in computed tomography-guided hook-wire localization versus electromagnetic navigation bronchoscopy-guided localization: a retrospective cohort study. *J Thorac Dis* 16:401–413. <https://doi.org/10.21037/jtd-23-1351>
28. Rostambeigi N, Scanlon P, Flanagan S, Frank N, Talaie R, Andrade R et al (2019) CT fluoroscopic-guided coil localization of lung nodules prior to video-assisted thoracoscopic surgical resection reduces complications compared to hook wire localization. *J Vasc Interv Radiol* 30:453–459. <https://doi.org/10.1016/j.jvir.2018.10.013>
29. Ali MS, Ghori UK, Wayne MT, Shostak E, De Cardenas J (2023) Diagnostic performance and safety profile of robotic-assisted bronchoscopy: a systematic review and meta-analysis. *Ann Am Thorac Soc* 20:1801–1812. <https://doi.org/10.1513/AnnalsATS.202301-075OC>
30. Anzidei M, Argirò R, Porfiri A, Boni F, Anile M, Zaccagna F et al (2015) Preliminary clinical experience with a dedicated interventional robotic system for CT-guided biopsies of lung lesions: a comparison with the conventional manual technique. *Eur Radiol* 25:1310–1316. <https://doi.org/10.1007/s00330-014-3508-z>

Publisher's Note Springer Nature remains neutral with regard to jurisdictional claims in published maps and institutional affiliations.